


Targeting tumor-infiltrating Ly6G⁺ myeloid cells improves sorafenib efficacy in mouse orthotopic hepatocellular carcinoma

Chun-Jung Chang ¹, Yao-Hsu Yang², Chiao-Juno Chiu³, Li-Chun Lu^{1,4}, Chien-Chia Liao³, Cher-Wei Liang^{5,8}, Chih-Hung Hsu^{1,4} and Ann-Lii Cheng^{1,4,6,7}

¹ Graduate Institute of Oncology, National Taiwan University College of Medicine, Taipei, Taiwan

² Department of Pediatrics, National Taiwan University Hospital, Taipei, Taiwan

³ Graduate Institute of Immunology, National Taiwan University College of Medicine, Taipei, Taiwan

⁴ Department of Oncology, National Taiwan University Hospital, Taipei, Taiwan

⁵ Graduate Institute of Pathology, National Taiwan University College of Medicine, Taipei, Taiwan

⁶ Department of Internal Medicine, National Taiwan University Hospital, Taipei, Taiwan

⁷ National Taiwan University Cancer Center, National Taiwan University College of Medicine, Taipei, Taiwan

⁸ Division of Pathology, Fu Jen Catholic University Hospital, New Taipei City, Taiwan

Sorafenib, a multikinase inhibitor with antiangiogenic activity, is an approved therapy for hepatocellular carcinoma (HCC). It is unclear whether the proinflammatory and immunosuppressive mechanisms may limit the therapeutic efficacy of sorafenib in HCC. We used a syngeneic mouse liver cancer cell line to establish orthotopic liver or subcutaneous tumors to study how proinflammatory and immunosuppressive mechanisms impact on the efficacy of sorafenib. We found sorafenib exhibited a potent therapeutic effect in subcutaneous tumors, but a less potent effect in orthotopic liver tumors. The protein levels of interleukin-6 (IL-6) and vascular endothelial growth factor A (VEGF-A) were persistently elevated in orthotopic liver tumors, but not in subcutaneous tumors, treated with sorafenib. Likewise, the tumor-infiltrating Ly6G⁺ myeloid-derived suppressor cells (MDSCs) and immune suppressors were increased in orthotopic liver tumors, not in subcutaneous tumors, treated with sorafenib. The tumor-infiltrating Ly6G⁺ MDSCs of sorafenib-treated orthotopic liver tumors significantly induced IL-10 and TGF- β expressing CD4⁺ T cells, and downregulated the cytotoxic activity of CD8⁺ T cells. IL-6, but not VEGF-A, protected Ly6G⁺ MDSCs from sorafenib-induced cell death *in vitro*. The combination of anti-Ly6G antibody or anti-IL-6 antibody with sorafenib significantly reduced the cell proportion of Ly6G⁺ MDSCs in orthotopic liver tumors, enhanced the T cells proliferation and improved the therapeutic effect of sorafenib synergistically. Modulating tumor microenvironment through targeting tumor-infiltrating Ly6G⁺ MDSCs represents a potential strategy to improve the anti-HCC efficacy of sorafenib.

Hepatocellular carcinoma (HCC) is an important malignant disease worldwide, especially in East Asian and African countries.¹ Sorafenib, a multikinase inhibitor with antiangiogenic activity by targeting vascular endothelial growth factor receptor (VEGFR), platelet-derived growth factor, and Raf kinase,²

is currently the most widely used systemic therapy for advanced HCC.^{3,4} However, the clinical efficacy of sorafenib against HCC is modest. Many HCC patients either do not respond to sorafenib treatment or have a short-lived disease stabilization. Previous studies have focused on the activation

Key words: multikinase inhibitor, tumor microenvironment, interleukin 6, Ly6G⁺ myeloid-derived suppressor cells

Additional Supporting Information may be found in the online version of this article.

Conflict of interest: Ann-Lii Cheng: consulting for Sanofi-Aventis, Pfizer, Bayer Schering Pharma, Bristol-Myers Squibb, Boehringer Ingelheim (Taiwan), and Novartis; Chih-Hung Hsu: consulting for Exelixis, Novartis, and Roche. The other authors declare no conflict of interests related to this article.

Grant sponsor: Ministry of Science and Technology, Executive Yuan, Taiwan; **Grant numbers:** MOST 103-2314-B-002-091, MOST 104-2314-B-002-077, MOST 105-2314-B-002-180; **Grant sponsor:** National Taiwan University Hospital; **Grant numbers:** NTUH 102-S2129, NTUH 103-S2359, NTUH 104-S2698; **Grant sponsor:** National Science Council; **Grant numbers:** NSC 101-2314-B-002-162, NSC 102-2314-B-002-144

DOI: 10.1002/ijc.31216

History: Received 13 June 2017; Accepted 24 Nov 2017; Online 20 Dec 2017

Correspondence to: Chih-Hung Hsu, M.D., Ph.D., Graduate Institute of Oncology, National Taiwan University College of Medicine, and Department of Oncology, National Taiwan University Hospital, 7 Chung-Shan South Road, Taipei 10002, Taiwan, E-mail: chihhunghsu@ntu.edu.tw; Tel: +886 2 23123456 ext. 67680, Fax: +886 2 23711174 or Ann-Lii Cheng, M.D., Ph.D., Department of Oncology and Department of Internal Medicine, National Taiwan University Hospital, 7 Chung-Shan South Road, Taipei 10002, Taiwan, E-mail: alcheng@ntu.edu.tw; Tel: +886 2 23123456 ext. 67251, Fax: +886 2 23711174

What's new?

The multi-kinase inhibitor sorafenib is an approved agent for the treatment of liver cancer. Using a syngeneic mouse liver cancer model, the authors found less therapeutic efficacy of sorafenib in orthotopic liver tumors as compared to subcutaneous tumors. They attributed this to increased levels of proinflammatory cytokines and immunosuppressive myeloid-derived suppressor cells found in orthotopic tumors, conditions that when suppressed increased sorafenib's therapeutic efficiency. The authors propose targeting the immunosuppressive tumor microenvironment as a novel therapeutic approach for liver cancers.

of alternative or parallel proangiogenic pathways to VEGF/VEGFR signaling such as the fibroblastic growth factor receptor (FGFR) signaling in mediating resistance to sorafenib.^{5–8} Other mechanisms contributing to sorafenib resistance have been under active investigation.

Myeloid-derived suppressor cells (MDSCs) are a heterogeneous population of cells that are defined by their myeloid lineage, immature status and immunosuppressive ability; they have been demonstrated to play significant roles in immunosuppression, proangiogenesis and tumor progression.^{9–14} MDSCs have also been shown to mediate resistance to antiangiogenic therapies in preclinical studies of various cancer types.^{15,16}

Several studies have reported that sorafenib could enhance the antitumor immunity by modulating MDSCs in preclinical models of HCC.^{17,18} However, Chen *et al.*¹⁹ demonstrated that sorafenib increased the infiltration of Gr1⁺ MDSCs through the interaction of stromal-derived factor-1 (SDF-1) and CXCR4 receptor type 4 in an orthotopic mouse liver cancer model. They also showed that myeloid differentiation antigen (Gr-1)⁺ MDSCs promoted tumor fibrosis and contributed to a decreased efficacy of sorafenib.¹⁹

In the current study, we used a syngeneic mouse liver cancer model to study the significance of tumor-infiltrating MDSCs in affecting the therapeutic effect of sorafenib. We found that the tumor-infiltrating MDSCs were increased in orthotopic liver tumors treated with sorafenib, and the immunosuppressive property of the tumor-infiltrating Ly6G⁺ MDSCs could attenuate the therapeutic effect of sorafenib. We also demonstrated that antibody-mediated therapy targeting Ly6G⁺ MDSCs or interleukin (IL)-6 improved the efficacy of sorafenib against liver cancer.

Material and Methods**Cell lines, animals and tumor model**

BNL, a mouse liver cancer cell line (ATCC TIB-75) kindly provided by Professor Lih-Hwa Hwang (National Yang-Ming University, Taipei, Taiwan)²⁰ was used to generate syngeneic mouse liver cancers in immunocompetent mice. Six-week-old male BALB/cByJNarl mice, purchased from the National Laboratory Animal Center (Taipei, Taiwan), were used in these experiments. T-cell receptor (TCR) transgenic mice DO11.10 (H-2d) bearing the TCR-recognized ovalbumin (OVA)_{323–339} peptide were kindly provided by Professor Bor-Luen Chiang (National Taiwan University Hospital, Taipei, Taiwan). To generate orthotopic liver cancers, we directly inoculated BNL

cells into the livers of BALB/cByJNarl mice as previously described.²⁰ All animal experiments were performed according to the guidelines of the Animal Care and Use Committee of the National Taiwan University College of Medicine.

Sorafenib treatment *in vivo*

Seven days or 14 days after the tumor cells were implanted in the liver or subcutaneous tissue, respectively, mice were orally fed with sorafenib (LC Laboratories, Woburn, MA) at the doses of 5 mg/kg/day or its solvent vehicle (Cremophor EL/95% ethanol in 50:50; Sigma-Aldrich, St. Louis, MO) daily for 1 or 3 weeks. Combination therapies were performed by administering sorafenib or vehicle control combined with neutralizing antibodies targeting Ly6G or IL-6 (i.e., anti-mouse Ly6G Ab or anti-mouse IL-6 Ab, respectively) or their corresponding isotype control antibodies (Bio X Cell, West Lebanon, NH). Antibody-based therapeutics were commenced from the fourth day after tumor cell implantation, with a loading dose of 25 mg/kg administered intraperitoneally (ip) followed by 4 mg/kg ip every 3 days for a total of seven doses. At the end of the experiments, the mice were sacrificed. Tumors were excised from the liver and weighed to obtain their mass (g).

Cell isolation

The mice were sacrificed to collect tumors, livers, spleens, femurs and tibias (for bone marrow [BM]) to enrich leukocytes by employing methods described previously.^{20,21} Whole blood (WB), collected through cardiac puncture, was suspended with an ammonium-chloride-potassium buffer to lyse red blood cells.

Flow cytometry

Leukocytes isolated from different tissues or T cells activated through *in vitro* stimulation were analyzed using surface marker staining alone or combined with intracellular cytokine staining by adopting methods described previously²⁰ to identify different cell subsets and their cytokine presentation. The antibodies used in our study are described in the Supporting Information Material section.

Cytospin and morphology analysis

Tumor-infiltrating leukocytes (TILs) were isolated as previously described and were then processed using the mouse MDSC isolation kit (Miltenyi Biotec GmbH, Bergisch Gladbach, Germany) to separate the Gr-1^{high} Ly6G⁺ myeloid cells

from the Gr-1^{dim} Ly6G⁻ myeloid cells for the subsequent experiments. The TILs were analyzed using cytospin by employing a Shandon Cytospin III centrifuge (Thermo Fisher Scientific, Inc., Rockford, IL). Cells were immediately stained with Liu's staining,²² and cell morphology was examined using a Zeiss Axio Observer D1 microscope and analyzed using AxioVision software (Carl Zeiss, Chester, VA).

Cytokine detection

Cytokines were isolated from tumor tissues according to a previously described method.²³ A cytokine bead array (BD Biosciences Pharmingen, San Jose, CA) was applied to analyze levels of IL-1 β , IL-3, IL-4, IL-5, IL-6, IL-12, IL-13 and TNF α . The amount of VEGF, SCF, G-CSF or TGF- β was determined using ELISA kits (Peprotech, Rocky Hill, NJ) according to the manufacturer's instructions. The concentration of each protein was normalized with the total protein determined using a bicinchoninic acid (BCA) protein analysis kit (Thermo Fisher Scientific).

Immunosuppression analysis of Ly6G⁺ MDSCs

The immunosuppression of Ly6G⁺ MDSCs was analyzed using T-cell proliferation, immunosuppressive CD4⁺ T-cell induction and cytotoxic CD8⁺ T-cell suppression. Employing methods, described previously,²⁰ were detailed in the Supporting Information Material section.

Quantitative real-time reverse-transcriptase polymerase chain reaction

Purified Ly6G⁺ MDSCs were homogenized in TRIzol reagent (Invitrogen), and total RNA was extracted and treated using a TURBO DNA-free kit to remove contaminated genomic DNA according to the manufacturer's instructions. Subsequently, reverse transcription was performed using Prime-Script RT master mix (Takara Bio, Kyoto, Japan) to determine relative quantities of mRNA. TaqMan Master Mix Premix *Ex Taq* (Takara Bio) and predesigned primers and fluorescein-labeled probe sets were used in our study and are described in the Supporting Information Material section.

In vitro culture of Ly6G⁺ MDSCs from mouse BM

Ly6G⁺ cells were isolated from BM of liver tumors-bearing mice treated with vehicle, followed by purification of Ly6⁺ cells. These BM-derived Ly6⁺ cells were cultured *in vitro* with BNL tumor cells in the presence or absence of various treatments such as IL-6 or VEGF-A for 5 days before assays.

Statistical analysis

Data are obtained from ≥ 3 independent experiments unless otherwise specified and are expressed as mean \pm standard deviations. The statistical testing was examined by two-tailed unpaired *t*-test or one-sample *t*-test using the Statistical Package of GraphPad Prism PRISM 5.0 (GraphPad Software, Inc, San Diego, CA). Statistical significance was marked as * when $p < 0.05$, ** when $p < 0.01$ and *** when $p < 0.001$.

Results

Therapeutic effect of sorafenib was less potent in orthotopic mouse liver tumors than in subcutaneous tumors

To monitor the effect of sorafenib in suppressing liver cancer growth, we treated the BNL mouse orthotopic liver tumors or subcutaneous tumors from the 8th day or 14th day after implanting tumor cells for 1–3 weeks (Fig. 1a). We found that sorafenib exhibited antitumor effects in both models. However, the therapeutic effects of sorafenib were more potent in subcutaneous BNL tumors than in orthotopic liver tumors. As shown in Figure 1b, subcutaneous tumors treated with sorafenib at the dose of 5 mg/kg/day were effectively suppressed through the treatment course, with the tumor burden ratios (the tumor weight of mice treated with sorafenib divided by that of mice treated with the vehicle) of 0.26 ± 0.02 at 1 week of sorafenib treatment and 0.19 ± 0.02 at the 3 week of sorafenib treatment, respectively. On the other hand, the tumor burden ratios of orthotopic liver tumors treated with sorafenib were 0.39 ± 0.12 at 1 week of sorafenib treatment and 0.70 ± 0.15 at 3 week of sorafenib treatment, respectively. These data suggested that the therapeutic effect of sorafenib was partially attenuated in orthotopic liver tumors compared to tumors established subcutaneously.

The orthotopic mouse liver tumors treated with sorafenib expressed increased levels of proinflammatory and immunosuppressive cytokines

To study whether inflammation and immunosuppression might have occurred and contributed to the less effectiveness of sorafenib in mouse orthotopic liver tumors, we analyzed the expression levels of a panel of inflammatory cytokines and soluble factors in liver tumor tissues treated with sorafenib or the vehicle (Fig. 1c, Supporting Information Fig. 1). We found that IL-6 and VEGF-A were persistently elevated in liver tumors treated with sorafenib from 1 week of treatment to the end of 3 week treatment (Fig. 1c). In addition, TGF- β , a well-known growth factor involving in tumor progression and immunosuppression, was significantly increased at 1 week of treatment, and trended to increase at 3 week of treatment (Fig. 1c). On the contrary, the levels of IL-6, VEGF-A and TGF- β did not increase in subcutaneous tumors treated with sorafenib (Fig. 1c).

The microenvironment of the orthotopic mouse liver tumors treated with sorafenib became toward immunosuppressive

We continued investigating whether the immunosuppressive microenvironment might underlie the differential efficacies of sorafenib in orthotopic and subcutaneous tumor models by characterizing their TILs. At 1 week after treated with sorafenib or vehicle in orthotopic tumor models, we observed both immune effector cells (including the CD4⁺ or CD8⁺ IFN- γ -

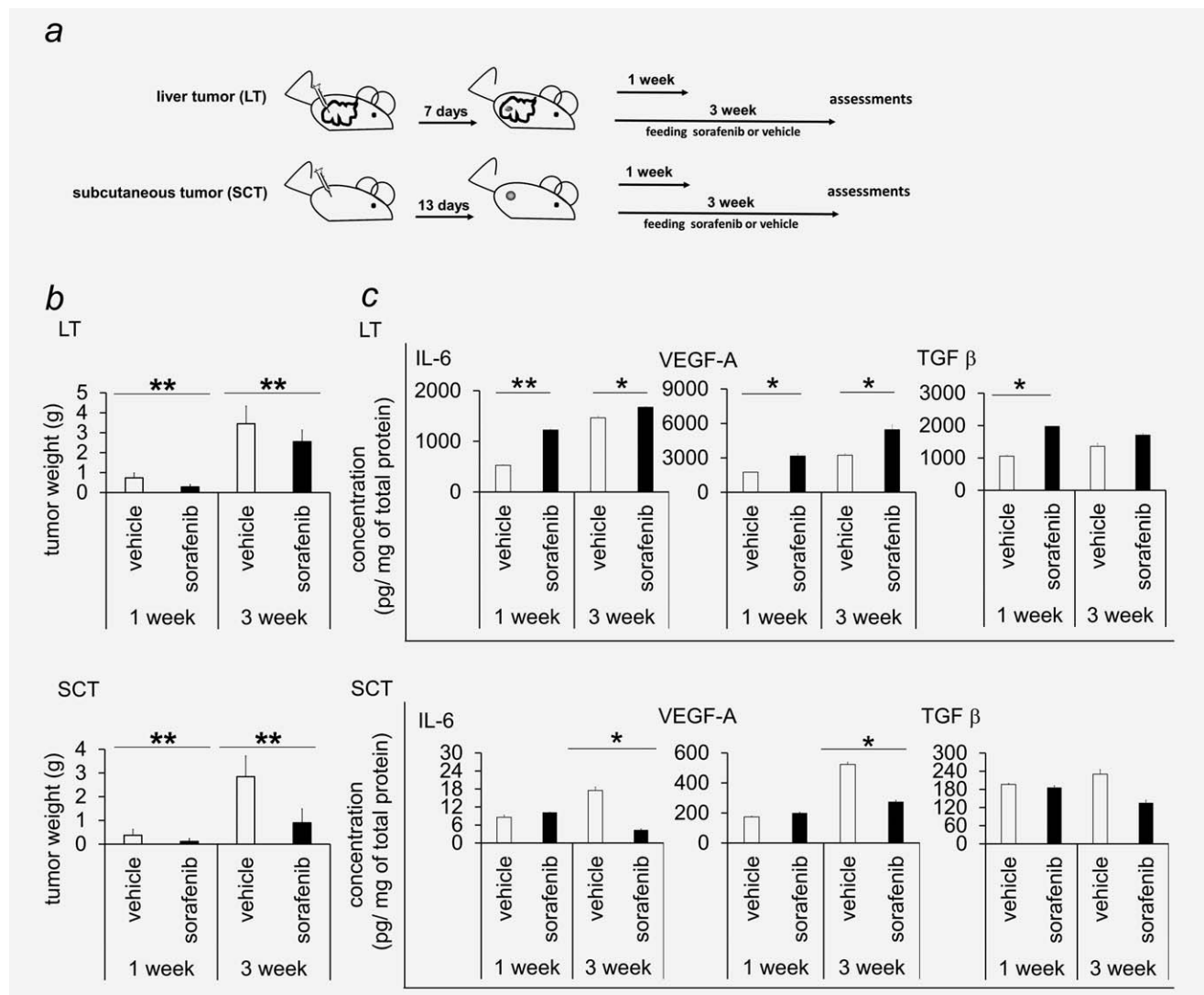


Figure 1. Sorafenib exhibited antitumor effects in orthotopic liver tumors and subcutaneous tumors of BNL mouse liver cancer cells. (a) Scheme of BALB/c mice, implanted with BNL mouse liver cancer cells in liver or subcutaneously, treated with sorafenib for 1 or 3 weeks. (b) Tumor weights of orthotopic liver tumors (LTs) or subcutaneous tumors (SCTs) treated with sorafenib at the dose of 5 mg/kg/day or vehicle for 1 and 3 weeks (number of mice per group, $N = 5$). (c) Protein levels of IL-6, VEGF-A or TGF- β of orthotopic LTs or SCTs treated with sorafenib or vehicle for 1 or 3 weeks ($n = 5$).

expressing T cell) and immunosuppressors (including the IL-10 or TGF- β -expressing CD4⁺ T cell and forkhead box P3 [FOXP3]-expressing CD4⁺ T cell) significantly increased in sorafenib-treated liver tumors (Fig. 2a). On the other hand, in subcutaneous liver tumor models, we found that most subsets of TILs were not significantly different between sorafenib-treated and vehicle-treated subcutaneous liver tumors except the TGF- β -expressing CD4⁺ T cells (Supporting Information Fig. 2A). We calculated the ratio of total immune effectors versus total immunosuppressors and found that this total effector-to-suppressor ratio was significantly lower in the orthotopic liver tumors treated with sorafenib than those treated with the vehicle (Fig. 2b). The total effector-to-suppressor ratio was not decreased in

subcutaneous tumors treated by sorafenib (Supporting Information Fig. 2B). To further confirm that this decreased effector-to-suppressor ratio in orthotopic liver tumors treated with sorafenib conferred an immunosuppressive status, we studied T-cell proliferation ability of TILs. As shown in Figure 2c significantly decreased T-cell proliferation stimulated by anti-CD3 and anti-CD28 antibodies was observed in the TILs isolated from sorafenib-treated liver tumors than those from vehicle-treated liver tumors. By contrast, the T-cell proliferation was significantly higher in the TILs isolated from sorafenib-treated subcutaneous tumors than those from vehicle-treated subcutaneous tumors (Supporting Information Fig. 2C). These data indicated that the microenvironment in orthotopic liver tumors, but not in subcutaneous tumors,

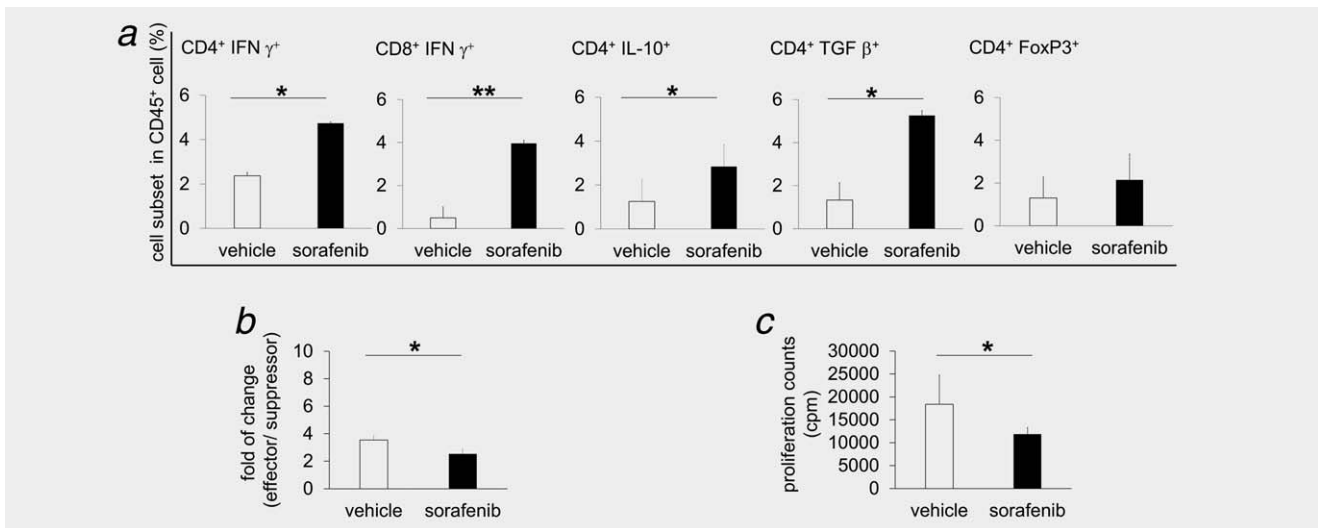


Figure 2. The tumor microenvironment of orthotopic mouse liver tumors treated with sorafenib tilted toward immunosuppression. (a) In orthotopic liver tumor models treated with sorafenib or vehicle for 1 week, tumor-infiltrating leukocytes were isolated and analyzed for the percentages of CD4⁺ IFN- γ -expressing T cells, or CD8⁺ IFN- γ -expressing T cells, IL-10-expressing CD4⁺ T cells, TGF- β -expressing CD4⁺ T cells and FOXP3-expressing CD4⁺ T cells (number of experiments, $n = 5$). (b) The ratio of total immune effectors versus total immunosuppressors was calculated by the sum of immune effector cells (including the CD4⁺ or CD8⁺ IFN- γ -expressing T cell) divided by the sum of immunosuppressors (including the IL-10 or TGF- β -expressing CD4⁺ T cell and FOXP3-expressing CD4⁺ T cell) in sorafenib- or vehicle-treated liver tumors ($n = 5$). (c) T-cell proliferation ability, stimulated by anti-CD3 and anti-CD28 antibodies and ³H-thymidine incorporation, in the presence of the TILs isolated from orthotopic liver tumors treated with sorafenib or vehicle ($n = 5$).

tilted toward immunosuppression following treatment with sorafenib.

Ly6G⁺ MDSCs increased significantly in the orthotopic liver tumors treated with sorafenib for 1 week

In studying the possible cellular mechanisms contributing to the immunosuppressive microenvironment of orthotopic liver tumors treated with sorafenib, we found that the proportion of CD11b⁺Gr-1⁺ MDSCs increased significantly in orthotopic liver tumors of sorafenib-treated mice compared to the vehicle-treated group (Fig. 3a). By cytospin and morphology analysis, we characterized that the majority of these MDSCs were Ly6G⁺ and Ly6C^{low}, the so-called PMN type of MDSCs (Fig. 3b) cells. In contrast, when we evaluated the frequencies of Ly6G⁺ MDSCs in the subcutaneous model, we observed a decrease of Ly6G⁺ MDSCs in the sorafenib-treated BNL tumors compared to vehicle-treated tumors (Fig. 3c). We also found that the expression levels of multiple genes involved in immunosuppression, including Arg I, NOS2, S100a8 and S100a9 (S100 calcium-binding protein A8/9), were increased in the Ly6G⁺ MDSCs isolated from the liver tumors treated with sorafenib compared to those treated with the vehicle. In addition, the transcript of signal transducer and activator of transcription (Stat)3 was consistently increased in the Ly6G⁺ MDSCs from sorafenib-treated tumors (Fig. 3d). These results indicated that the Ly6G⁺ MDSCs, expressing immunosuppressive characteristics, were the major subset of MDSCs accumulating in the orthotopic liver tumors treated with sorafenib.

Ly6G⁺ MDSCs from liver tumors of sorafenib-treated mice induced immunosuppression by inhibiting T-cell functions

We isolated the Ly6G⁺ MDSCs from orthotopic liver tumors treated with sorafenib and investigated their immunosuppressive effect on CD4⁺ and CD8⁺ T cell functions. In the assay of CD4⁺ T-cell activation through OVA-specific peptide stimulation, we found that the Ly6G⁺ MDSCs isolated from the liver tumors of the sorafenib-treated mice significantly induced immunosuppressive IL-10-expressing, TGF- β -expressing, but not FOXP3-expressing CD4⁺ T cells (Fig. 4a). In addition, the frequency of IFN- γ -expressing CD4⁺ T cells decreased (Figs. 4a and 4b), and CD4⁺ T-cell proliferation was inhibited (Fig. 4c) when cocultured with these Ly6G⁺ MDSCs. In assaying CD8⁺ T cell function, we stimulated tumor antigen-specific-CD8⁺ T cells in the presence of tumor-derived MDSCs. We found that tumor-derived Ly6G⁺ MDSCs suppressed the induction of IFN- γ -expressing, granzyme-expressing and perforin-expressing CD8⁺ T cells (Fig. 4d) and inhibited the tumoricidal effect of CD8⁺ T cells analyzed by killing of tumor antigen-specific target cells (Fig. 4e). These data suggested that Ly6G⁺ MDSCs derived from the liver tumors of the sorafenib-treated mice exhibited immunosuppression by inducing an immunosuppressive population from CD4⁺ T cells and suppressing the functions of effector T cells.

IL-6 signaling provided a key survival signal to sorafenib-triggered cell death and promoted immunosuppressive function in Ly6G⁺ MDSCs

IL-6 and VEGF-A have been shown to promote expansion and proliferation of MDSCs in tumors.²⁴ In our mouse liver

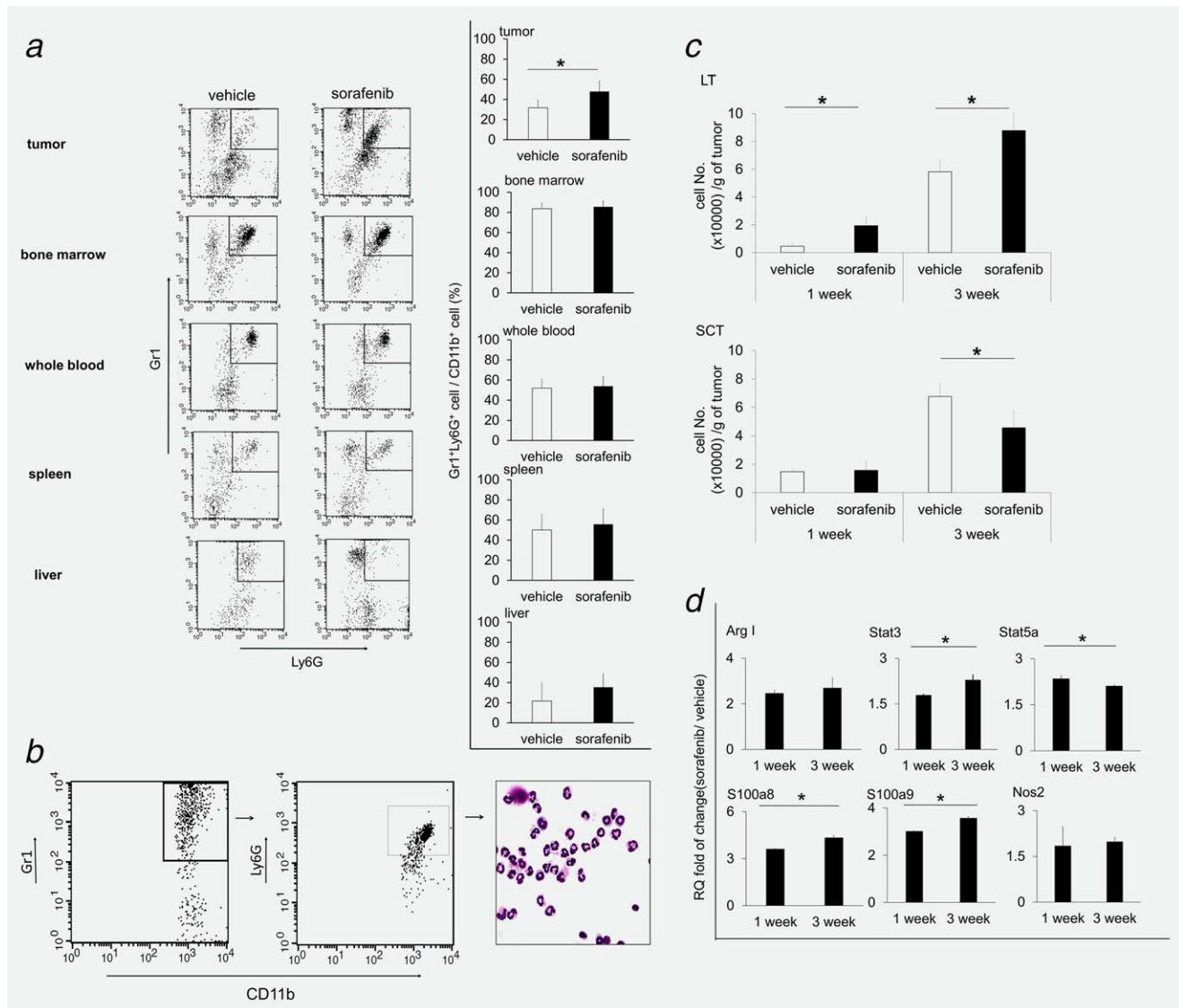


Figure 3. A significant increase of Ly6G⁺ MDSCs in orthotopic mouse liver tumors treated with sorafenib. (a) The frequencies of Ly6G⁺ MDSCs in total CD11b⁺ cells isolated from various organs and liver tumors from mice treated with sorafenib or vehicle for 1 week. Data shown are from a representative experiment. (b) Characterization of Ly6G⁺ MDSCs as the dominant subtype of the TILs increased in sorafenib-treated mice. Data shown are from a representative experiment. (c) The quantitation of Ly6G⁺ MDSCs, total cell number per gram of orthotopic liver tumors (LT) or subcutaneous tumors (SCT) obtained from mice treated with sorafenib or the vehicle for 1 or 3 weeks (number of experiments, $n = 3-5$). (d) Transcriptional levels of Arg1, nitric oxide synthase 2, S100A8/9, Stat5a and Stat3 were detected by using Taqman-based real-time RT-PCR analysis in the Ly6G⁺ MDSCs isolated from mouse liver tumors treated with sorafenib or vehicle for 1 or 3 weeks ($n = 3$). Data are presented as the folds of change calculated from the expression levels of indicated gene of sorafenib-treated group relative to those from the vehicle-treated group ($n = 3$). [Color figure can be viewed at wileyonlinelibrary.com]

cancer model, we found that the expression levels of IL-6 receptors (CD126, CD130 and the soluble forms of IL-6R α) and VEGFR2 were significantly increased on the Ly6G⁺ MDSCs of orthotopic liver tumors treated with sorafenib (Supporting Information Figs. 3A and 3B). We also found that Ly6G⁺ MDSCs of orthotopic liver tumors treated with sorafenib exhibited an increase of p-Stat3 expression, indicating an activation of IL-6 downstream JAK/Stat signaling in the Ly6G⁺ MDSCs (Fig. 5b). In cultured Ly6G⁺ MDSCs treated with sorafenib, the presence of IL-6 abolished the sorafenib-mediated downregulation of p-Stat3, whereas the

Ly6G⁺ MDSCs, we studied the viability and cell signaling of the *in vitro* cultured BM-derived Ly6G⁺ MDSCs treated with sorafenib (Fig. 5a). We found that IL-6 at the doses of 5 or 10 ng/mL effectively protected Ly6G⁺ MDSCs from cell death induced by sorafenib, quantitated by 7AAD and Annexin V staining (Fig. 5b). By contrast, VEGF up to 10 ng/mL did not abrogate the cell death induced by sorafenib in the Ly6G⁺ MDSCs (Fig. 5b). In cultured Ly6G⁺ MDSCs treated with sorafenib, the presence of IL-6 abolished the sorafenib-mediated downregulation of p-Stat3, whereas the

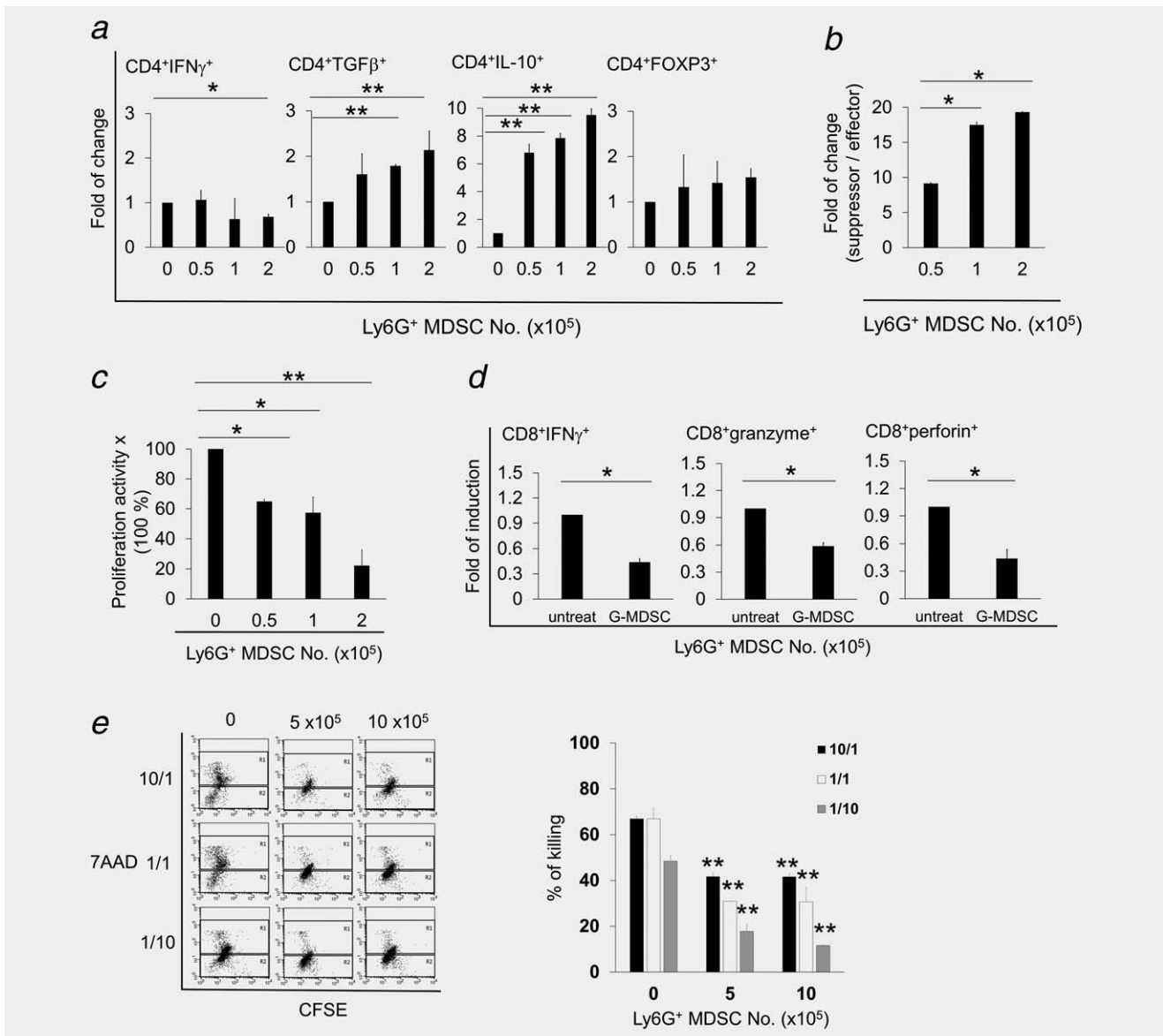


Figure 4. The Ly6G⁺ MDSCs from mouse liver tumors treated with sorafenib suppressed T cell functions. (a–c) CD4⁺ T cell function assays through OVA-specific peptide activation: In the presence of 0–2 × 10⁵ Ly6G⁺ MDSCs, the CD4⁺T cell were analyzed for the expression of IFN- γ , TGF- β , IL-10 and FOXP3 (a) (number of experiments, $n = 3–5$). The ratios of total analyzed suppressive CD4⁺T cells versus IFN- γ -expressing CD4⁺T cells were shown in (b) ($n = 3–5$). The T-cell proliferation, assayed 48 hr after OVA-specific activation followed by ³H-thymidine incorporation analysis, was expressed in the ratios normalized to untreated controls (c) ($n = 3–5$). (d, e) CD8⁺ T cell function assays through the stimulation of tumor antigens: In the presence of 1 × 10⁵ Ly6G⁺ MDSCs, the CD8⁺T cell were analyzed for the expression of IFN- γ , granzyme and perforin (d) ($n = 3$). The killing function of tumor antigen-specific CD8⁺ T cells, assayed by coculture of CFSE-labeled tumor cells with antigen-specific CD8⁺ T cells and Ly6G⁺ MDSCs in different combination ratios for 6–7 hr, was determined by 7AAD staining (e, left panel) and quantitated after normalized with untreated controls (e, right panel) ($n = 3$). Data shown are from a representative experiment.

presence of VEGF-A only partially attenuated the sorafenib-induced p-VEGFR2 downregulation (Supporting Information Fig. 7). Regarding the immunosuppressive functions of Ly6G⁺ MDSCs, we found that the BM-derived Ly6G⁺ MDSCs preconditioned with IL-6 (10 ng/mL) for 5 days exhibited a dose-dependent inhibitory effect in CD4⁺ T-cell proliferation activated by anti-CD3 Ab and anti-CD28 Ab (Supporting

Information Figs. 4A and 4B), and dose-dependently increased the proportions of IL-10-expressing and TGF- β -expressing CD4⁺ T cells (Supporting Information Figs. 4C and 4D). These data indicated that the high intratumor IL-6 not only provided Ly6G⁺ MDSCs in mouse liver tumors the survival signal to the proapoptotic effect of sorafenib but also promoted their immunosuppressive functions.

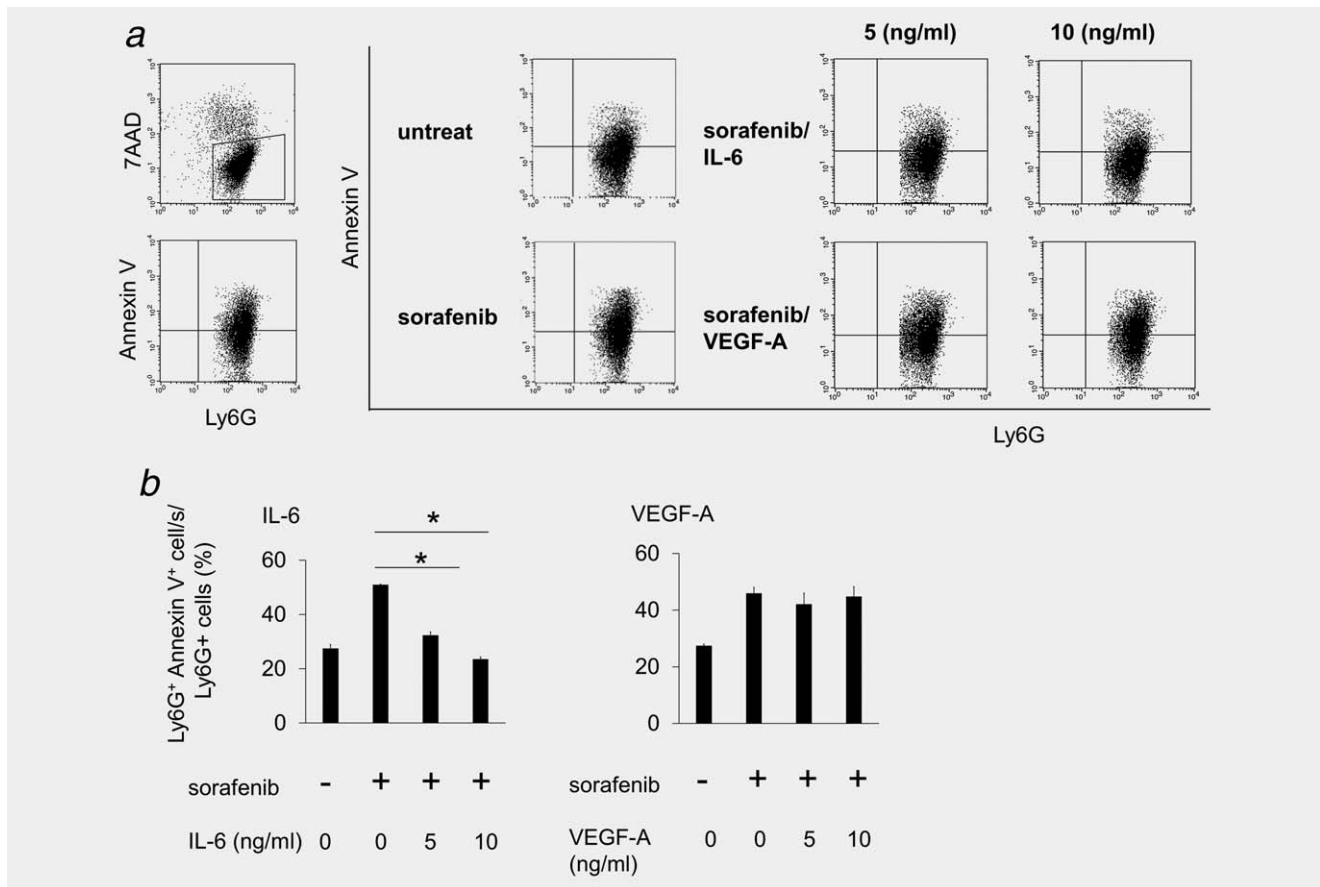


Figure 5. IL-6 protected Ly6G⁺ MDSCs from sorafenib-induced cell death. The viability of BM-derived MDSCs treated with 2.5 μ M of sorafenib, in the presence of IL-6 or VEGF-A, evaluated by Annexin V and 7AAD staining (number of experiments, $n = 3$). Data shown are from a representative experiment.

Sorafenib combined with anti-Ly6G Ab or anti-IL-6 Ab improved the therapeutic effect of sorafenib in the orthotopic liver tumors

To confirm that Ly6G⁺ MDSCs indeed played a critical role in attenuating the therapeutic efficacy of sorafenib in orthotopic liver tumors, we first tested the effect of depleting Ly6G⁺ MDSCs by an anti-mouse Ly6G Ab in orthotopic mouse liver cancer model treated with sorafenib. The combination of anti-mouse Ly6G Ab plus sorafenib, compared to isotype Ab plus sorafenib or anti-mouse Ly6G plus vehicle, resulted in a significantly lower tumor burden (Fig. 6a). The combination of anti-Ly6G Ab plus sorafenib yielded the lowest frequency of Ly6G⁺ MDSCs in TILs from the liver tumors and in splenocytes (Figs. 6b and 6h), improved the immunosuppressive status indicated by the highest T-cell proliferation activity using TILs (Fig. 6c) and significantly decreased the protein levels of IL-6 and TGF- β , but not VEGF-A, in liver tumors (Fig. 6g). We subsequently tested the efficacy of targeting IL-6 combined with sorafenib in the orthotopic liver tumor models. The combination of anti-IL-6 Ab plus sorafenib was significantly more potent in suppressing the liver tumor growth than other treatment groups (Fig. 6d). The combination of anti-IL-6 Ab plus sorafenib yielded the lowest frequency of Ly6G⁺ MDSCs in TILs from the liver tumors

and in splenocytes (Figs. 6e and 6h), improved the immunosuppressive status with the highest T-cell proliferation activity using TILs (Fig. 6f) and significantly decreased the protein levels of IL-6, VEGF-A and TGF- β in liver tumors (Fig. 6g). On detailed evaluation of the characteristics of T cells in mouse liver tumors, we also found that the combination of anti-IL-6 Ab plus sorafenib yielded higher proportion of Ki-67-expressing CD8⁺ T cells than other treatment groups, higher proportion of Tbet⁺ Eomes⁻ CD8⁺ effector T cells than sorafenib treatment group, and higher IFN- γ -expressing CD4⁺ T cells and IFN- γ -expressing CD8⁺ T cells than other treatment groups (Supporting Information Figs. 5A–5C). Using a luciferase-expressing mouse liver cancer model, we also observed the improved therapeutic efficacy of combining sorafenib with anti-IL-6 Ab (Supporting Information Figs. 5D–5F). Overall, these data demonstrated that the targeting of the tumor microenvironment by anti-IL-6 Ab improved the therapeutic efficacy of sorafenib through modulating the immunosuppressive functions of Ly6G⁺ MDSCs in orthotopic mouse liver tumors.

Discussion

In the current study, using syngeneic BNL mouse liver cancer model, we demonstrated the Ly6G⁺ MDSC was the major

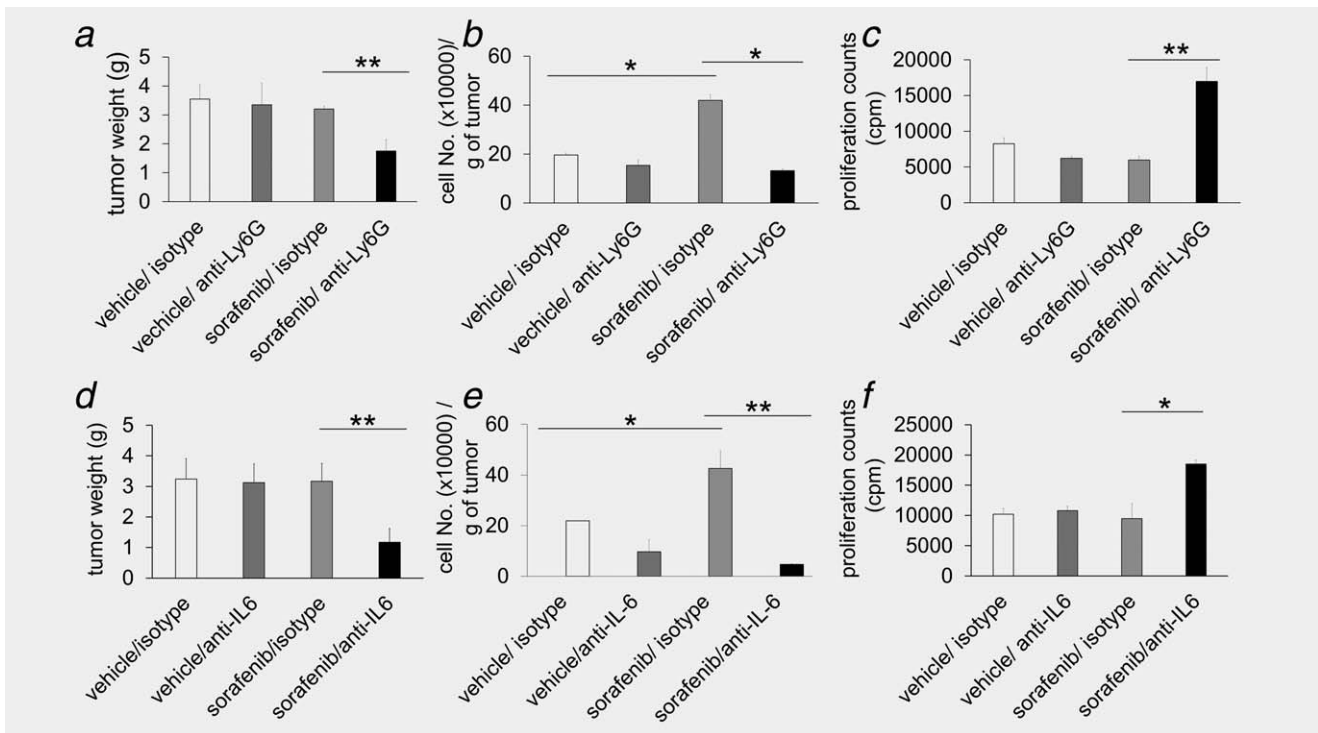


Figure 6. The combination of sorafenib with anti-Ly6G Ab or anti-IL-6 Ab exhibited improved antitumor effects against orthotopic mouse liver tumors. (a–c) Orthotopic BNL mouse liver tumors treated with sorafenib or vehicle plus anti-Ly6G Ab or isotype Ab: tumors weight after treatment for 3 weeks (a) (number of mice per group, $N = 5$), numbers of Ly6G⁺ MDSCs isolated from liver tumors (b) (number of experiments, $n = 3$) and T-cell proliferation activated by anti-CD3 Ab and anti-CD28 Ab followed by ³H-thymidine incorporation (c) (number of experiment, $n = 3$). (d–f) Orthotopic BNL mouse liver tumor treated with sorafenib or vehicle plus anti-IL-6 Ab or isotype Ab: tumors weight after treatment for 3 weeks (d) ($n = 3$), numbers of Ly6G⁺ MDSCs isolated from liver tumors (e) (number of experiments, $n = 3$) and T-cell proliferation activated by anti-CD3 Ab and anti-CD28 Ab followed by ³H-thymidine incorporation (f) ($n = 3$). (g) Protein levels of IL-6, VEGF-A or TGF- β were detected in orthotopic liver tumors treated with sorafenib plus anti-Ly6G Ab or isotype Ab (upper panel), or sorafenib plus anti-IL6 Ab or isotype Ab for 3 weeks ($n = 9$). (h) Orthotopic BNL mouse liver tumors treated with sorafenib or vehicle plus anti-Ly6G Ab (left panel) or anti-IL6 Ab (right panel) or their respective isotype Ab, splenocytes were isolated for determining the numbers of Ly6G⁺ MDSCs ($n = 3$).

subtype of tumor-infiltrating MDSCs and contributed to a less effectiveness of sorafenib in orthotopic liver tumors than in subcutaneous tumors through promoting an immunosuppressive tumor microenvironment. In addition, we showed that Ly6G⁺ MDSCs depletion by anti-Ly6G Ab or anti-IL-6 Ab improved the therapeutic efficacy of sorafenib in orthotopic mouse liver tumors.

In the current study, we found that the persistent increase of IL-6, VEGF-A and TGF- β occurred in orthotopic BNL mouse liver tumors treated with sorafenib, but not in subcutaneous tumors treated with sorafenib. Our observation may suggest that the induction of proinflammatory, proangiogenic or immunosuppressive cytokines in response to sorafenib treatment could be tumor microenvironment specific. In a preliminary data using another mouse liver tumor model ML-1_{4a},²⁵ we also found that the protein levels of IL-6 and VEGF-A were increased in orthotopic liver tumors treated with sorafenib but not in subcutaneous tumors (Supporting Information Fig. 6). However, many cell lineages in liver and HCC microenvironment have been reported to be able to

produce inflammatory cytokines and proangiogenic factors to promote tumor progression, such as Kupffer cells, myeloid cells, tumor-associated macrophages and others.^{14,26,27} Further studies are warranted to identify the cell types responsible for IL-6 and VEGF production in HCC microenvironment after sorafenib treatment so that the potential cellular targets can be further explored to improve the therapeutic efficacy of sorafenib.

Previous studies have revealed that sorafenib may augment antitumor immunity by reducing regulatory T cells or CD11b⁺Gr-1⁺ MDSCs in tumor-bearing mice.^{17,28} However, in our study, while we also found the number of Ly6G⁺ MDSCs was decreased in subcutaneous tumors treated with sorafenib (Fig. 3c), we observed that the Ly6G⁺ MDSCs number was significantly increased in orthotopic liver tumors treated with sorafenib. Our observations imply that the role of Ly6G⁺ MDSCs is microenvironment-dependent. Our data showing the increase of tumor-infiltrating Ly6G⁺ MDSCs was inversely associated with the efficacy of sorafenib is line with a recent publication of Zhou *et al.*²⁶ who

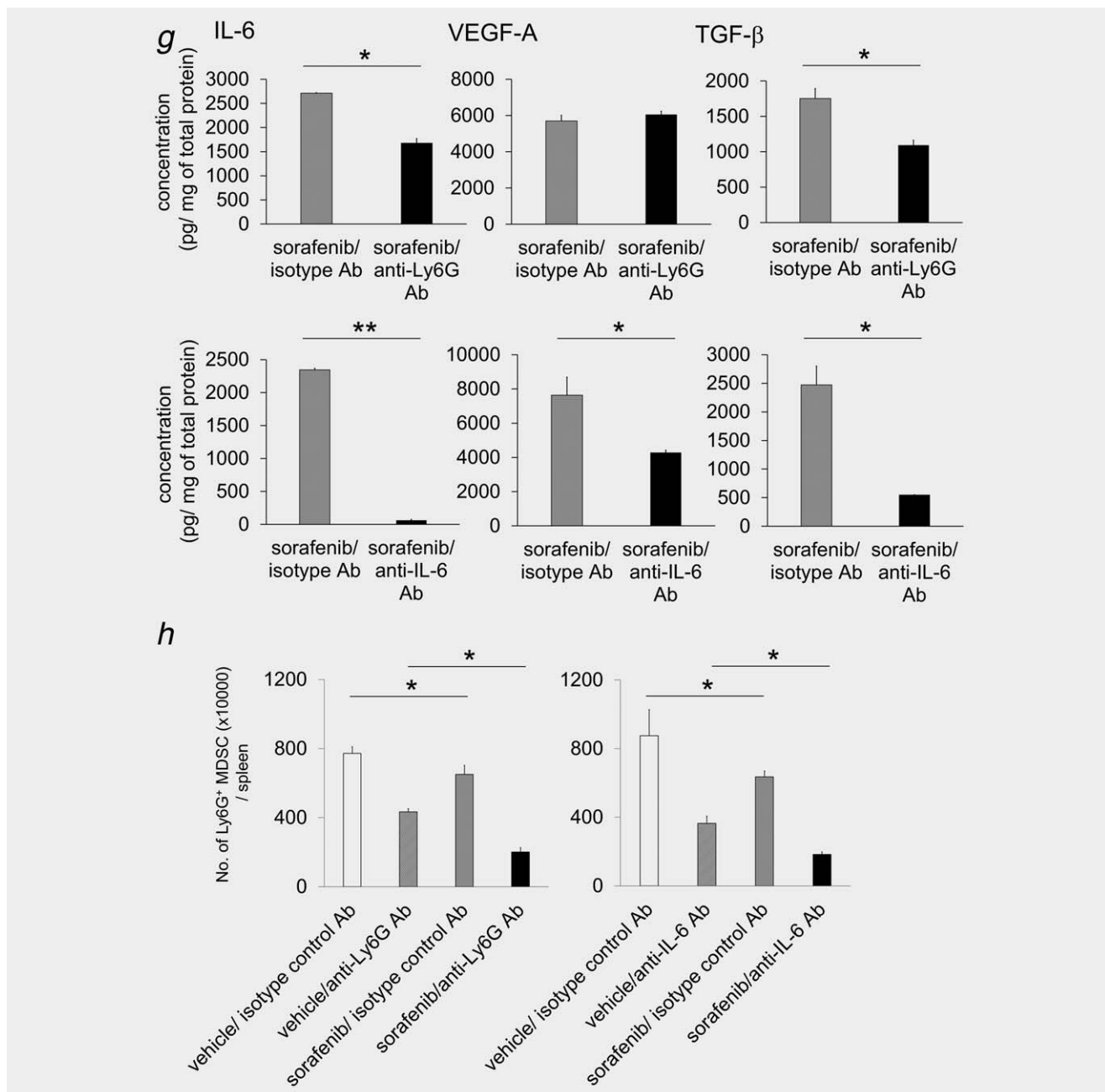


Figure 6. Continued.

demonstrated that PMN-type cells involved in the resistance to sorafenib using preclinical liver cancer models and human HCC samples.

The well-known immunosuppressive mechanisms of Ly6C^{high} Ly6G^{-dim} M-MDSC and Ly6C^{-dim} Ly6G^{high} G-MDSCs include the production of NO (nitric oxide), ROS (reactive oxygen species), Arg I or NADPH oxidase 2 (NOX2) to suppress T-cell function.^{12,29} Other immunosuppressive actions of MDSCs involve IL-10 or TGF-β-expressing CD4⁺ T cells conversion, FOXP3-expressing regulatory T cell differentiation and expansion, and induction of CD8⁺ T-cell tolerance.³⁰⁻³⁶ In our study, we found that the

sorafenib-treated liver tumor-derived Ly6G⁺ MDSCs were capable of inducing IL-10-expressing and TGF-β-expressing CD4⁺ T cells in specific Ag-induced T-cell activation *ex vivo* (Fig. 4).

Expression of G-CSF, Bv8, IL-8, hypoxia-inducing factor 1α and SDF-1 has been demonstrated to mobilize CD11b⁺Gr-1⁺ MDSCs into tumor microenvironment to promote tumor progression.^{9,11} Previous studies have also revealed that IL-6 participates in MDSCs expansion²⁴ and MDSCs transmigration in hypoxic tumor microenvironment.³⁷ IL-6 is a pleiotropic inflammatory cytokine that participates in multiple normal physiological functions³⁸ and

plays an important role in promoting tumor progression^{39,40} through Stat3-dependent signaling pathway.⁴¹ In our study, we demonstrated that IL-6 (Fig. 1c) was elevated in orthotopic liver tumors treated with sorafenib, the expression levels of IL-6 receptors and the downstream p-Stat 3 were significantly increased in Ly6G⁺ MDSCs isolated from orthotopic liver tumors treated with sorafenib (Supporting Information Fig. 3) and IL-6 provided survival signals to sorafenib-induced apoptosis in cultured Ly6G⁺ MDSCs (Fig. 5). Our data support the critical role of IL-6 signaling in the expansion, survival, and functioning of the tumor-infiltrating Ly6G⁺ MDSCs in attenuating the therapeutic efficacy of sorafenib in orthotopic mouse liver tumors.

Recently, immunotherapy especially immune checkpoint blockade has emerged as a new paradigm of cancer therapy.⁴² In September 2017, the Food and Drug Administration of the United States granted an accelerated approval of nivolumab for HCC patients previously treated with sorafenib. Nivolumab, an antibody targeting programmed cell death protein 1 (PD-1) has been shown to exhibit an objective tumor response of 20% in advanced HCC patients.⁴³ The anti-IL-6 antibody-mediated sorafenib-sensitizing effect is

worthy of further clinical validation because several antibodies targeting IL-6/IL-6 receptor have been commercialized for treating human diseases.^{44,45} Furthermore, given the facts that both MDSCs and IL-6 play significant roles in promoting tumor growth through immunosuppression and angiogenesis, their roles in affecting the efficacy of immune checkpoint blockade as cancer therapy may warrant further investigations.

In conclusion, we demonstrated that sorafenib treatment was associated with an increase of proinflammatory cytokine IL-6 and immune suppressive Ly6G⁺ MDSCs in mouse liver tumors, and depleting tumor-infiltrating Ly6G⁺ MDSCs by anti-IL-6 or anti-Ly6G Abs improved the antitumor effect of sorafenib. Targeting tumor-infiltrating Ly6G⁺ MDSCs represents a potential strategy to improve the anti-HCC efficacy of sorafenib.

Acknowledgement

The authors appreciate Professor Manfred Lutz (Institute of Virology and Immunobiology, Würzburg University, Germany) for providing hybridoma cells to generate anti-Gr-1 Ab and for constructive discussion about MDSCs.

References

- Hernandez-Gea V, Toffanin S, Friedman SL, et al. Role of the microenvironment in the pathogenesis and treatment of hepatocellular carcinoma. *Gastroenterology* 2013;144:512–27.
- Wilhelm S, Carter C, Lynch M, et al. Discovery and development of sorafenib: a multikinase inhibitor for treating cancer. *Nat Rev Drug Discov* 2006;5:835–44.
- Llovet JM, Ricci S, Mazzaferro V, et al. Sorafenib in advanced hepatocellular carcinoma. *N Engl J Med* 2008;359:378–90.
- Cheng AL, Kang YK, Chen Z, et al. Efficacy and safety of sorafenib in patients in the Asia-Pacific region with advanced hepatocellular carcinoma: a phase III randomised, double-blind, placebo-controlled trial. *Lancet Oncol* 2009;10:25–34.
- Casanovas O, Hicklin DJ, Bergers G, et al. Drug resistance by evasion of antiangiogenic targeting of VEGF signaling in late-stage pancreatic islet tumors. *Cancer Cell* 2005;8:299–309.
- Kerbel RS. Therapeutic implications of intrinsic or induced angiogenic growth factor redundancy in tumors revealed. *Cancer Cell* 2005;8:269–71.
- Cheng AL, Shen YC, Zhu AX. Targeting fibroblast growth factor receptor signaling in hepatocellular carcinoma. *Oncology* 2011;81:372–80.
- Sampat KR, O'Neil B. Antiangiogenic therapies for advanced hepatocellular carcinoma. *Oncologist* 2013;18:430–8.
- Marigo I, Dolcetti L, Serafini P, et al. Tumor-induced tolerance and immune suppression by myeloid derived suppressor cells. *Immunol Rev* 2008;222:162–79.
- Yang L, DeBusk LM, Fukuda K, et al. Expansion of myeloid immune suppressor Gr⁺CD11b⁺ cells in tumor-bearing host directly promotes tumor angiogenesis. *Cancer Cell* 2004;6:409–21.
- Murdoch C, Muthana M, Coffelt SB, et al. The role of myeloid cells in the promotion of tumour angiogenesis. *Nat Rev Cancer* 2008;8:618–31.
- Talmadge JE, Gabrilovich DI. History of myeloid-derived suppressor cells. *Nat Rev Cancer* 2013;13:739–52.
- Greifengberg V, Ribechini E, Rößner S, et al. Myeloid-derived suppressor cell activation by combined LPS and IFN-gamma treatment impairs DC development. *Eur J Immunol* 2009;39:2865–76.
- Wan S, Kuo N, Kryczek I, et al. Myeloid cells in hepatocellular carcinoma. *Hepatology* 2015;62:1304–12.
- Finke JH, Rayman PA, Ko JS, et al. Modification of the tumor microenvironment as a novel target of renal cell carcinoma therapeutics. *Cancer J* 2013;19:353–64.
- Shojaei F, Wu X, Malik AK, et al. Tumor refractoriness to anti-VEGF treatment is mediated by CD11b⁺Gr1⁺ myeloid cells. *Nat Biotechnol* 2007;25:911–20.
- Cao M, Xu Y, Youn JI, et al. Kinase inhibitor Sorafenib modulates immunosuppressive cell populations in a murine liver cancer model. *Lab Invest* 2011;91:598–608.
- Kapanadze T, Gamrekelashvili J, Ma C, et al. Regulation of accumulation and function of myeloid derived suppressor cells in different murine models of hepatocellular carcinoma. *J Hepatol* 2013;59:1007–13.
- Chen Y, Huang Y, Reiberger T, et al. Differential effects of sorafenib on liver versus tumor fibrosis mediated by stromal-derived factor 1 alpha/C-X-C receptor type 4 axis and myeloid differentiation antigen-positive myeloid cell infiltration in mice. *Hepatology* 2014;59:1435–47.
- Chang CJ, Chen YH, Huang KW, et al. Combined GM-CSF and IL-12 gene therapy synergistically suppresses the growth of orthotopic liver tumors. *Hepatology* 2007;45:746–54.
- Chang CJ, Yang YH, Liang YC, et al. A novel phycobiliprotein alleviates allergic airway inflammation by modulating immune responses. *Am J Respir Crit Care Med* 2011;183:15–25.
- Lee CH, Lan RS, Tsai YH, et al. Riu's stain in the diagnosis of pulmonary cryptococcosis. Introduction of a new diagnostic method. *Chest* 1988;93:467–70.
- Ebos JM, Lee CR, Christensen JG, et al. Multiple circulating proangiogenic factors induced by sunitinib malate are tumor-independent and correlate with antitumor efficacy. *Proc Natl Acad Sci USA* 2007;104:17069–74.
- Condamine T, Gabrilovich DI. Molecular mechanisms regulating myeloid-derived suppressor cell differentiation and function. *Trends Immunol* 2011;32:19–25.
- Chang CP, Yang MC, Liu HS, et al. Concanavalin A induces autophagy in hepatoma cells and has a therapeutic effect in a murine in situ hepatoma model. *Hepatology* 2007;45:286–96.
- Zhou SL, Zhou ZJ, Hu ZQ, et al. Tumor-associated neutrophils recruit macrophages and T-regulatory cells to promote progression of hepatocellular carcinoma and resistance to sorafenib. *Gastroenterology* 2016;150:1646–58.
- Schmidt-Arras D, Rose-John S. IL-6 pathway in the liver: from physiopathology to therapy. *J Hepatol* 2016;64:1403–15.
- Chen ML, Yan BS, Lu WC, et al. Sorafenib relieves cell-intrinsic and cell-extrinsic inhibitions of effector T cells in tumor microenvironment to augment antitumor immunity. *Int J Cancer* 2014;134:319–31.
- Movahedi K, Williams M, Van den Bossche J, et al. Identification of discrete tumor-induced myeloid-derived suppressor cell subpopulations with distinct T cell-suppressive activity. *Blood* 2008;111:4233–44.
- Kusmartsev S, Nefedova Y, Yoder D, et al. Antigen-specific inhibition of CD8⁺ T cell response by immature myeloid cells in cancer is mediated

- by reactive oxygen species. *J Immunol* 2004;172:989–99.
31. Hoehchst B, Ormandy LA, Ballmaier M, et al. A new population of myeloid-derived suppressor cells in hepatocellular carcinoma patients induces D4(+)CD25(+)Foxp3(+) T cells. *Gastroenterology* 2008;135:234–43.
 32. Jitschin R, Braun M, Büttner M, et al. CLL-cells induce IDOhi CD14+HLA-DRlo myeloid-derived suppressor cells that inhibit T-cell responses and promote TRegs. *Blood* 2014;124:750–60.
 33. Huang B, Pan PY, Li Q, et al. 1+CD115+ immature myeloid suppressor cells mediate the development of tumor-induced T regulatory cells and T-cell anergy in tumor-bearing host. *Cancer Res* 2006;66:1123–31.
 34. Solito S, Bronte V, Mandruzzato S. Antigen specificity of immune suppression by myeloid-derived suppressor cells. *J Leukoc Biol* 2011;90:31–6.
 35. Nagaraj S, Nelson A, Youn JI, et al. Antigen-specific CD4(+) T cells regulate function of myeloid-derived suppressor cells in cancer via retrograde MHC class II signaling. *Cancer Res* 2012;72:928–38.
 36. Nagaraj S, Gupta K, Pisarev V, et al. Altered recognition of antigen is a mechanism of CD8+ T cell tolerance in cancer. *Nat Med* 2007;13:828–35.
 37. Hong J, Tobin NP, Rundqvist H, et al. Role of tumor pericytes in the recruitment of myeloid-derived suppressor cells. *JNCIJ* 2015;107:pii: djv209.
 38. Scheller J, Chalaris A, Schmidt-Arras D, et al. The pro- and anti-inflammatory properties of the cytokine interleukin-6. *Biochim Biophys Acta* 2011;1813:878–88.
 39. Tsukamoto H, Senju S, Matsumura K, et al. IL-6-mediated environmental conditioning of defective Th1 differentiation dampens antitumour immune responses in old age. *Nat Commun* 2015;6:6702.
 40. Trikha M, Corringham R, Klein B, et al. Targeted anti-interleukin-6 monoclonal antibody therapy for cancer: a review of the rationale and clinical evidence. *Clin Cancer Res* 2003;9:4653–65.
 41. Lee H, Pal SK, Reckamp K, et al. STAT3: a target to enhance antitumor immune response. *Curr Top Microbiol Immunol* 2011;344:41–59.
 42. Sharma P, Allison JP. Immune checkpoint targeting in cancer therapy: toward combination strategies with curative potential. *Cell* 2015;161:205–14.
 43. El-Khoueiry AB, Sangro B, Yau T, et al. Nivolumab in patients with advanced hepatocellular carcinoma (CheckMate 040): an open-label, non-comparative, phase 1/2 dose escalation and expansion trial. *Lancet* 2017;389:2492–502.
 44. Tanaka T, Kishimoto T. Targeting interleukin-6: all the way to treat autoimmune and inflammatory diseases. *Int J Biol Sci* 2012;8:1227–36.
 45. Rossi JF, Lu ZY, Jourdan M, et al. Interleukin-6 as a therapeutic target. *Clin Cancer Res* 2015;21:1248–57.